Correspondence

Estimating Directions of Arrival of Completely and Incompletely Polarized Signals with Electromagnetic Vector Sensors

Kwok-Chiang Ho, Kah-Chye Tan, and Arye Nehorai

***Abstract*—We are concerned with direction-of-arrival estimation and signal classification with electromagnetic vector sensors for scenarios where completely and incompletely polarized signals may co-exist. We propose an efficient ESPRIT-based method, address the identifiability of the proposed method, and compare its performance against CRB.**

***Index Terms*—Array signal processing, direction-of-arrival estimation, electromagnetic waves, polarization, vector sensors.**

I. Introduction

Electromagnetic (EM) vector sensors (VS's), which measure the complete electric and magnetic fields induced by EM signals at a point, have been shown to be very useful and effective for direction-of-arrival (DOA) estimation [1]–[8]. When the EM VS was first introduced, a cross-product-based DOA estimation method applicable to single-source scenarios was proposed (see [1] and [2]). Subsequently, three different ESPRIT-based methods for estimating the DOA's of multiple signals with an array of EM VS's have been developed separately via the work reported in [9]–[11], which we will refer to as ESPRIT1, ESPRIT2, and ESPRIT3, respectively. As a matter of fact, each of these three methods is applicable only to a specific type of EM signals: ESPRIT1 and ESPRIT2 are designed for only completely polarized (CP) signals, whereas ESPRIT3 for only incompletely polarized (IP) signals. (The polarization state of a CP signal is constant, whereas that of an IP signal varies with time.) However, in some practical applications, such as DOA estimation on an airborne platform, both CP and IP signals may be encountered. Therefore, it is of theoretical interest and practical importance to develop DOA-estimation methods for scenarios where CP and IP signals co-exist.

Basically, an IP signal comprises two incoherent CP signals having the same DOA. Therefore, it is commonly thought that a DOA-estimation method designed for CP signals can be directly applied for scenarios where CP and IP signals co-exist—for each IP signal, the method would simply give two DOA estimates having the same value, each of which corresponds to a CP signal belonging to the IP signal of concern. However, this common perception is not always true. In fact, it has been established analytically in [12] that the estimates obtained with ESPRIT1 would be practically unusable as long as an IP signal exists. Interestingly, ESPRIT3, which was customized for IP signals, would also produce unreliable results in the presence of CP signals.

Hence, we cannot take it for granted that a method devised based on CP (IP) signal model is automatically applicable to IP (CP) signals. On the contrary, a dedicated analysis must be devoted to investigating its applicability to the other types of signals. In this connection, we investigate whether ESPRIT2 can be used for DOA estimation in cases where both CP and IP signals co-exist. Our investigation indicates that ESPRIT2, with an additional assumption (additional in the sense that it was not mentioned in [10]) and some extra processing, can be used in the presence of both CP and IP signals. Actually, ESPRIT2 is customized for use with a specific three-sensor array. This motivates us to carry out an appropriate generalization so that ESPRIT2, with some appropriate modifications we will introduce later on, becomes applicable to more types of three-sensor arrays, as well as a class of arrays with arbitrary number of sensors. For convenience, we will refer to ESPRIT2 with the additional assumption, processing, and modifications we introduce as ESPRIT2$'$.

We also present a fairly thorough analysis of the identifiability of ESPRIT2$'$ and assess its performance via a comparison of the root-mean-square errors of the estimates with a Cramér-Rao bound (CRB) related expression.

II. Preliminary Discussion

A. Data Model

Ferrara and Parks [14] have studied the use of diversely polarized sensors (cross dipoles in particular) for estimating the DOA's of CP signals. Here, we will use the notation of Ferrara and Parks [14] with an appropriate modification so that it is applicable to EM VS's receiving both CP and IP signals. The modification is basically on the expression of the steering vectors—we adopt the one proposed in [1], which is suitable for both CP and IP signals.

Consider an array of m EM VS's receiving n EM signals at time t, and let the azimuth and elevation of the kth signal be $\phi_k \in (-\pi, \pi]$ and $\theta_k \in [-\pi/2, \pi/2]$, respectively. The measurement received at the array can be model as

$$\boldsymbol{y}(t) = \boldsymbol{A}\boldsymbol{\rho}(t) + \boldsymbol{e}(t) \tag{2.1}$$

where $\boldsymbol{y}(t)$ and $\boldsymbol{e}(t)$ are $6m \times 1$ complex vectors, respectively, given by

$$\begin{aligned}
\boldsymbol{y}(t) &= [\boldsymbol{y}_{\mathrm{e}}^{(1)}(t), \boldsymbol{y}_{\mathrm{h}}^{(1)}(t), \cdots, \boldsymbol{y}_{\mathrm{e}}^{(m)}(t), \boldsymbol{y}_{\mathrm{h}}^{(m)}(t)]^T \in \mathbb{C}^{6m\times 1}\\
\boldsymbol{e}(t) &= [\boldsymbol{e}_{\mathrm{e}}^{(1)}(t), \boldsymbol{e}_{\mathrm{h}}^{(1)}(t), \cdots, \boldsymbol{e}_{\mathrm{e}}^{(m)}(t), \boldsymbol{e}_{\mathrm{h}}^{(m)}(t)]^T \in \mathbb{C}^{6m\times 1}\\
\boldsymbol{A} &= [\boldsymbol{v}_\phi(\phi_1,\theta_1), \boldsymbol{v}_\theta(\phi_1,\theta_1), \cdots, \boldsymbol{v}_\phi(\phi_n,\theta_n)\\
&\qquad \boldsymbol{v}_\theta(\phi_n,\theta_n)] \in \mathbb{C}^{6m\times 2n}\\
\boldsymbol{v}_\phi(\phi_k,\theta_k) &= \boldsymbol{d}(\phi_k,\theta_k) \otimes \boldsymbol{v}_\phi^{(\circ)}(\phi_k,\theta_k) \in \mathbb{C}^{6m\times 1}\\
\boldsymbol{v}_\theta(\phi_k,\theta_k) &= \boldsymbol{d}(\phi_k,\theta_k) \otimes \boldsymbol{v}_\theta^{(\circ)}(\phi_k,\theta_k) \in \mathbb{C}^{6m\times 1}\\
\boldsymbol{v}_\phi^{(\circ)}(\phi_k,\theta_k) &= [-\sin\phi_k, \cos\phi_k, 0, -\cos\phi_k \sin\theta_k\\
&\qquad -\sin\phi_k\sin\theta_k, \cos\theta_k]^T \in \Re^{6\times 1}
\end{aligned}$$

Manuscript received April 25, 1997; revised on February 18, 1999. The work of A. Nehorai was supported by the Air Force Office of Scientific Research under Grants F49620-97-1-0481 and F49620-99-1-0067, the National Science Foundation under Grant MIP-9615590, and the Office of Naval Research under Grant N00014-98-1-0542. The associate editor coordinating the review of this paper and approving it for publication was Prof. José M. F. Moura.

K.-C. Ho and K.-C. Tan are with the Centre for Signal Processing, School of Electrical and Electronic Engineering, Nanyang Technological University, Republic of Singapore.

A. Nehorai is with the Department of Electrical Engineering and Computer Science, the University of Illinois at Chicago, Chicago, IL 60607-7053 USA.

Publisher Item Identifier S 1053-587X(99)07660-6.

$$\begin{aligned}
\boldsymbol{v}_\theta^{(\circ)}(\phi_k,\theta_k) &= [-\cos\phi_k\sin\theta_k, -\sin\phi_k\sin\theta_k \\
&\qquad \cos\theta_k, \sin\phi_k, -\cos\phi_k, 0]^T \in \Re^{6\times 1} \\
\boldsymbol{d}(\phi_k,\theta_k) &= [e^{j2\pi \boldsymbol{u}(\phi_k,\theta_k)\bullet \boldsymbol{r}_1/\lambda}, \cdots \\
&\qquad e^{j2\pi \boldsymbol{u}(\phi_k,\theta_k)\bullet \boldsymbol{r}_m/\lambda}]^T \in \mathbb{C}^{m\times 1} \\
\boldsymbol{u}(\phi_k,\theta_k) &= [u_k^x, u_k^y, u_k^z]^T \\
&= [\cos\phi_k\cos\theta_k, \sin\phi_k\cos\theta_k, \sin\theta_k]^T \in \Re^{3\times 1} \\
\boldsymbol{\rho}(t) &= [\boldsymbol{\rho}_1^T(t), \cdots, \boldsymbol{\rho}_n^T(t)]^T \in \mathbb{C}^{2n\times 1} \\
\boldsymbol{\rho}_k(t) &= [\rho_\phi(\gamma_k,\eta_k,t), \rho_\theta(\gamma_k,\eta_k,t)]^T \in \mathbb{C}^{2\times 1}.
\end{aligned}$$

Here

- $\otimes$ Kronecker product operator;
- $\bullet$ dot product operator;
- ^{T} transpose operator.

The vectors $\boldsymbol{y}_{\rm e}^{(l)}(t) \in \mathbb{C}^{1\times 3}$ and $-\boldsymbol{y}_{\rm h}^{(l)}(t)/r \in \mathbb{C}^{1\times 3}$ are, respectively, the three-component measurements of the electric and magnetic fields at the lth sensor at time t, where r is the intrinsic impedance of the medium, and $\boldsymbol{e}_{\rm e}^{(l)}(t) \in \mathbb{C}^{1\times 3}$ and $\boldsymbol{e}_{\rm h}^{(l)}(t) \in \mathbb{C}^{1\times 3}$ are, correspondingly, the noise components in the measurements. The vectors $\boldsymbol{v}_\phi(\phi_k,\theta_k)$ and $\boldsymbol{v}_\theta(\phi_k,\theta_k)$ are the responses of the array due to an EM wave coming from direction (ϕ_k,θ_k) with linear polarizations along, respectively, the ϕ-direction and the θ-direction. The vectors $\boldsymbol{v}_\phi^{(\circ)}(\phi_k,\theta_k)$ and $\boldsymbol{v}_\theta^{(\circ)}(\phi_k,\theta_k)$ have the same meanings as $\boldsymbol{v}_\phi(\phi_k,\theta_k)$ and $\boldsymbol{v}_\theta(\phi_k,\theta_k)$, respectively, except that they correspond to responses of one EM VS. The two entries of the vector $\boldsymbol{\rho}_k(t)$ represent the complex envelopes of the kth transmitted signal, the lth entry of $\boldsymbol{d}(\phi_k,\theta_k)$ denotes the phase delay of the kth signal at the lth sensor with respect to the origin, λ represents the wavelength of the signals, and $\boldsymbol{r}_l$ denotes the coordinates of the lth sensor. The vector $-\boldsymbol{u}(\phi_k,\theta_k)$ is the normalized Poynting vector (PV) of the kth signal.

The rank of the covariance matrix of the kth signal $\boldsymbol{R}_{\boldsymbol{\rho}_k} \triangleq E(\boldsymbol{\rho}_k(t)\boldsymbol{\rho}_k^H(t))$ is related to the polarization state of the kth signal, where 'E' and '^{H}' are, respectively, the expectation and hermitian operators (see [15]). Indeed, if $\boldsymbol{R}_{\boldsymbol{\rho}_k}$ is of full rank, then the signal is IP, and its polarization varies with time. On the other hand, if $\boldsymbol{R}_{\boldsymbol{\rho}_k}$ is rank deficient, then the signal is CP, and it has constant polarization. Note that for CP signal, $\boldsymbol{\rho}_k(t)$ can be expressed as $[\cos\gamma_k, \sin\gamma_k e^{j\eta_k}]^T s_k(t)$, where $\gamma_k \in [0,\pi/2]$ and $\eta_k \in (-\pi,\pi]$ are polarization parameters referred as the auxiliary polarization angle and polarization phase difference, respectively, and $s_k(t)$ the complex envelope of the kth signal. Thus, the response of the array due to a CP signal $[\boldsymbol{v}_\phi(\phi_k,\theta_k),\ \boldsymbol{v}_\theta(\phi_k,\theta_k)]\boldsymbol{\rho}_k$, can be compactly expressed as

$$[\boldsymbol{v}_\phi(\phi_k,\theta_k), \boldsymbol{v}_\theta(\phi_k,\theta_k)]\boldsymbol{\rho}_k = \boldsymbol{v}(\boldsymbol{\Psi}_k)s_k(t) \tag{2.2}$$

where

$$\begin{aligned}
\boldsymbol{v}(\boldsymbol{\Psi}_k) &= \boldsymbol{d}(\phi_k,\theta_k) \otimes \boldsymbol{v}^{(\circ)}(\boldsymbol{\Psi}_k), \quad \boldsymbol{\Psi}_k = (\phi_k,\theta_k,\gamma_k,\eta_k) \\
\boldsymbol{v}^{(\circ)}(\boldsymbol{\Psi}_k) &\triangleq [\boldsymbol{v}_\phi^{(\circ)}(\phi_k,\theta_k), \boldsymbol{v}_\theta^{(\circ)}(\phi_k,\theta_k)]\begin{pmatrix}\cos\gamma_k \\ \sin\gamma_k e^{j\eta_k}\end{pmatrix}.
\end{aligned} \tag{2.3}$$

The vector $\boldsymbol{v}(\boldsymbol{\Psi}_k)$ with parameter $\boldsymbol{\Psi}_k = (\phi_k,\theta_k,\gamma_k,\eta_k)$ is the steering vector of the array associated with a CP signal coming from the direction (ϕ_k,θ_k) with polarization (γ_k,η_k), and the matrix $[\boldsymbol{v}_\phi(\phi_k,\theta_k), \boldsymbol{v}_\theta(\phi_k,\theta_k)]$ is the steering matrix of the array associated with an IP signal with DOA (ϕ_k,θ_k). Note that $\boldsymbol{v}^{(\circ)}(\boldsymbol{\Psi}_k)$ is the steering vector of one EM VS associated with a CP signal with parameter $\boldsymbol{\Psi}_k$, and the matrix $[\boldsymbol{v}_\phi^{(\circ)}(\phi_k,\theta_k),\ \boldsymbol{v}_\theta^{(\circ)}(\phi_k,\theta_k)]$ is the steering matrix of one EM VS associated with an IP signal with parameter $(\phi_k,\ \theta_k)$.

Without loss of generality, assume that the first p signals are CP, and the remaining q signals are IP (thus the total number of signals is $n = p + q$). Then, we obtain from (2.1) and (2.2) the array measurements as follows:

$$\boldsymbol{y}(t) = \boldsymbol{A}\boldsymbol{z}(t) + \boldsymbol{e}(t) \tag{2.4}$$

where

$$\begin{aligned}
\boldsymbol{A} &= [\boldsymbol{v}(\boldsymbol{\Psi}_1), \cdots, \boldsymbol{v}(\boldsymbol{\Psi}_p), \boldsymbol{v}_\phi(\phi_{p+1},\theta_{p+1}) \\
&\qquad \boldsymbol{v}_\theta(\phi_{p+1},\theta_{p+1}), \cdots, \boldsymbol{v}_\phi(\phi_{p+q},\theta_{p+q}) \\
&\qquad \boldsymbol{v}_\theta(\phi_{p+q},\theta_{p+q})] \in \mathbb{C}^{6m\times(p+2q)} \\
\boldsymbol{z}(t) &= [s_1(t), \cdots, s_p(t), \boldsymbol{\rho}_{p+1}(t), \cdots, \boldsymbol{\rho}_{p+q}(t)]^T \in \mathbb{C}^{(p+2q)\times 1}.
\end{aligned}$$

For convenience, we will hereafter use $\boldsymbol{v}_k$, $\boldsymbol{v}_k^{(\circ)}$, $\boldsymbol{v}_{\phi,k}$, $\boldsymbol{v}_{\theta,k}$, $\boldsymbol{v}_{\phi,k}^{(\circ)}$, $\boldsymbol{v}_{\theta,k}^{(\circ)}$, $\boldsymbol{d}_k$, and $\boldsymbol{u}_k$ to denote, respectively, $\boldsymbol{v}(\boldsymbol{\Psi}_k)$, $\boldsymbol{v}^{(\circ)}(\boldsymbol{\Psi}_k)$, $\boldsymbol{v}_\phi(\phi_k,\theta_k)$, $\boldsymbol{v}_\theta(\phi_k,\theta_k)$, $\boldsymbol{v}_\phi^{(\circ)}(\phi_k,\theta_k)$, $\boldsymbol{v}_\theta^{(\circ)}(\phi_k,\theta_k)$, $\boldsymbol{d}(\phi_k,\theta_k)$ and $\boldsymbol{u}(\phi_k,\theta_k)$.

B. Basic Assumptions and Preliminary Discussion

Now, we will establish some useful relationships between the eigenvectors of the array covariance matrix and the steering vectors of the array for the case where CP and IP signals co-exist. First, we make the following assumptions that are essential for ESPRIT2 and ESPRIT2$'$.

- Assumption 1) The DOA's $(\phi_1,\theta_1), \cdots, (\phi_n,\theta_n)$ are pairwise distinct.
- Assumption 2) The signals are incoherent (i.e., $E(z(t)z^H(t))$ is of full rank).
- Assumption 3) The signals are uncorrelated with the noise.
- Assumption 4) The noise covariance matrix is a constant multiple of the identity matrix.
- Assumption 5) The columns of the matrix $[\boldsymbol{v}(\hat{\boldsymbol{\Psi}}_1), \cdots, \boldsymbol{v}(\hat{\boldsymbol{\Psi}}_{n+1})]$ are linearly independent for all distinct DOA's $(\hat\phi_1,\hat\theta_1), \cdots, (\hat\phi_{n+1},\hat\theta_{n+1})$ and arbitrary polarizations $(\hat\gamma_1,\hat\eta_1), \cdots, (\hat\gamma_{n+1},\hat\eta_{n+1})$.

It follows from Assumptions 2)–4) and (2.4) that the array covariance matrix can be expressed as $\boldsymbol{R}_{\boldsymbol{y}} = E(\boldsymbol{y}(t)\boldsymbol{y}^H(t)) = \boldsymbol{A}\boldsymbol{R}_{\boldsymbol{z}}\boldsymbol{A}^H + \sigma^2\boldsymbol{I}_{6m}$, where $\boldsymbol{R}_{\boldsymbol{z}} = E(z(t)z^H(t))$ is nonsingular, and σ^2 is the noise power. Let the eigenvalues and the corresponding eigenvectors of $\boldsymbol{R}_{\boldsymbol{y}}$ be $\lambda_1, \cdots, \lambda_{6m}$ and $\boldsymbol{h}_1, \cdots, \boldsymbol{h}_{6m}$, respectively, and assume, without loss of generality, that $\lambda_1 \geq \cdots \geq \lambda_{6m}$. Then, it can be shown that $\lambda_1 \geq \lambda_2 \geq \cdots \geq \lambda_{p+2q} > \lambda_{p+2q+1} = \cdots = \lambda_{6m} = \sigma^2$ and that

$$\begin{aligned}
&\boldsymbol{A}^H\boldsymbol{E}_n = \boldsymbol{0}, \quad \text{where} \\
&\quad \boldsymbol{E}_n = [\boldsymbol{h}_{p+2q+1}, \cdots, \boldsymbol{h}_{6m}] \in \mathbb{C}^{6m\times(6m-p-2q)}.
\end{aligned} \tag{2.5}$$

Moreover, there exists a unique nonsingular matrix $\boldsymbol{T} \in \mathbb{C}^{(p+2q)\times(p+2q)}$ such that

$$\begin{aligned}
&\boldsymbol{E}_s\boldsymbol{T} = \boldsymbol{A}, \quad \text{where} \\
&\quad \boldsymbol{E}_s = [\boldsymbol{h}_1, \cdots, \boldsymbol{h}_{p+2q}] \in \mathbb{C}^{6m\times(p+2q)}.
\end{aligned} \tag{2.6}$$

Note that the columns of $\boldsymbol{E}_n$ are commonly referred to as noise eigenvectors, whereas those of $\boldsymbol{E}_s$ signal eigenvectors.

III. Analysis of ESPRIT2 and Details of ESPRIT2$'$

A. A Brief Discussion of ESPRIT2

We begin with a brief discussion of ESPRIT2 as proposed in [10] since this will facilitate the discussion of ESPRIT2$'$. In fact, ESPRIT2 makes use of a right-triangular array of three VS's with coordinates (0, 0, 0), (Δ, 0, 0) and (0, Δ, 0), where Δ can be larger than half wavelength. Two sets of PV estimates for the signals are first obtained, one of which is of *low variance but ambiguous*, whereas the other is *high variance but unambiguous*. Subsequently, a set of *low variance and unambiguous* PV estimates is obtained by combining the information extracted from the two sets. The DOA estimates of the signals can then be extracted from the PV estimates.

Since the work reported in [10] is concerned with only CP signals, the array measurement is given by (2.4) with $p = n$ and $q = 0$. Exploiting the fact that the array of concern is a three-sensor right-triangular array, (2.4) can be rewritten as

$$\begin{aligned}\boldsymbol{y}(t) &= \boldsymbol{A}\boldsymbol{z}(t) + \boldsymbol{e}(t)\\ &= [\boldsymbol{A}_\circ^T, (\boldsymbol{D}^x)^T\boldsymbol{A}_\circ^T, (\boldsymbol{D}^y)^T\boldsymbol{A}_\circ^T]^T\boldsymbol{z}(t) + \boldsymbol{e}(t) \in \mathbb{C}^{18\times 1}\end{aligned} \tag{3.1}$$

where

$$\begin{aligned}\boldsymbol{A}_\circ &= [\boldsymbol{v}_1^{(\circ)}, \cdots, \boldsymbol{v}_p^{(\circ)}] \in \mathbb{C}^{6\times p}\\ \boldsymbol{D}^x &= \text{Diag}\{e^{j2\pi\Delta u_1^x/\lambda}, \cdots, e^{j2\pi\Delta u_p^x/\lambda}\} \in \mathbb{C}^{p\times p}\\ \boldsymbol{D}^y &= \text{Diag}\{e^{j2\pi\Delta u_1^y/\lambda}, \cdots, e^{j2\pi\Delta u_p^y/\lambda}\} \in \mathbb{C}^{p\times p}.\end{aligned} \tag{3.2}$$

Now, we state a necessary assumption.

Assumption 6) The columns of the matrix $\boldsymbol{A}_\circ$ are linearly independent.

Let $\boldsymbol{\Gamma}^x$ and $\boldsymbol{\Gamma}^y$ be the matrices satisfying, respectively, $\boldsymbol{E}_{s,1}\boldsymbol{\Gamma}^x = \boldsymbol{E}_{s,2}$ and $\boldsymbol{E}_{s,1}\boldsymbol{\Gamma}^y = \boldsymbol{E}_{s,3}$, where $\boldsymbol{E}_{s,1}$, $\boldsymbol{E}_{s,2}$, and $\boldsymbol{E}_{s,3}$ are the matrices comprising the first six rows, the second six rows, and the last six rows of $\boldsymbol{E}_s$, respectively. Then, it follows from (2.6), (3.1), and Assumption 6 that

$$\boldsymbol{\Gamma}^x = \boldsymbol{T}\boldsymbol{D}^x\boldsymbol{T}^{-1} \quad \text{and} \quad \boldsymbol{\Gamma}^y = \boldsymbol{T}\boldsymbol{D}^y\boldsymbol{T}^{-1}. \tag{3.3}$$

Next, let the eigenvalues and a set of corresponding eigenvectors of $\boldsymbol{\Gamma}^x$ be $\{f_k | k = 1, \cdots n\}$ and $\{\boldsymbol{f}_k | k = 1, \cdots n\}$, respectively, and let the eigenvalues and a set of corresponding eigenvectors of $\boldsymbol{\Gamma}^y$ be $\{g_k | k = 1, \cdots n\}$ and $\{\boldsymbol{g}_k | k = 1, \cdots n\}$, respectively. Then, it follows from (3.3) that f_k and g_k, for $k = 1, \cdots, n$, are, respectively, equal to the diagonal elements of $\boldsymbol{D}^x$ and $\boldsymbol{D}^y$. Without loss of generality, assume that

$$f_k = d_k^x \qquad \text{and} \quad g_k = d_k^y, \quad \text{for } k = 1, \cdots, n \tag{3.4}$$

where d_k^x and d_k^y are, respectively, the kth diagonal elements of $\boldsymbol{D}^x$ and $\boldsymbol{D}^y$.

It can then be deduced from (3.2) and (3.4) that the candidates for u_k^x are given by the set S_k^x, and the candidates for u_k^y are given by the set S_k^y, where

$$\begin{aligned}S_k^x &= \left\{\frac{\lambda}{\Delta}\left(\mu + \frac{\angle f_k}{2\pi}\right) \middle| \mu \in \boldsymbol{Z}, \left|\frac{\lambda}{\Delta}\left(\mu + \frac{\angle f_k}{2\pi}\right)\right| \le 1\right\}\\ S_k^y &= \left\{\frac{\lambda}{\Delta}\left(\nu + \frac{\angle g_k}{2\pi}\right) \middle| \nu \in \boldsymbol{Z}, \left|\frac{\lambda}{\Delta}\left(\nu + \frac{\angle g_k}{2\pi}\right)\right| \le 1\right\}\end{aligned} \tag{3.5}$$

$\boldsymbol{Z}$ is the set of all integers, and $\angle f_k$ and $\angle g_k$ are the principal arguments of f_k and g_k, respectively. A set of *low variance but ambiguous* PV estimates for the kth signal is then given by

$$S_k = \{(a, b, \pm\sqrt{1 - a^2 - b^2})^T | a \in S_k^x, b \in S_k^y, a^2 + b^2 \le 1\}. \tag{3.6}$$

(Note that the pairing of the eigenvalues of $\boldsymbol{\Gamma}^x$ and $\boldsymbol{\Gamma}^y$ can be accomplished using the method suggested in [10].)

Assume that $\boldsymbol{f}_k$ is a scalar multiple of the kth column of $\boldsymbol{T}$, as in (2.6), for $k = 1, \cdots, n$. Then, it can be deduced from (2.6) that the kth column of $\boldsymbol{A}_\circ$ is a scalar multiple of the kth column of the matrix

$$\hat{\boldsymbol{A}}_\circ \triangleq \boldsymbol{E}_{s,1}\boldsymbol{F} \tag{3.7}$$

where $\boldsymbol{F} = [\boldsymbol{f}_1, \cdots, \boldsymbol{f}_n]$. Now, let us denote the top 3×1 subvectors and the bottom 3×1 subvectors of the kth column of $\hat{\boldsymbol{A}}_\circ$ as $\hat{\boldsymbol{A}}_{\circ,k}^{(\mathrm{e})}$ and $\hat{\boldsymbol{A}}_{\circ,k}^{(\mathrm{h})}$, respectively. Then, the cross product of $\hat{\boldsymbol{A}}_{\circ,k}^{(\mathrm{e})}/\|\hat{\boldsymbol{A}}_{\circ,k}^{(\mathrm{e})}\|$ and $\hat{\boldsymbol{A}}_{\circ,k}^{(\mathrm{h})}/\|\hat{\boldsymbol{A}}_{\circ,k}^{(\mathrm{h})}\|$ (which are, respectively, the electric field vector and magnetic field vector of the kth signal) yields the PV estimate for the kth signal, which is of *high variance but unambiguous*

$$-\hat{\boldsymbol{u}}(\phi_k, \theta_k) = -\text{Re}\{\hat{\boldsymbol{A}}_{\circ,k}^{(\mathrm{e})}/\|\hat{\boldsymbol{A}}_{\circ,k}^{(\mathrm{e})}\| \times (\hat{\boldsymbol{A}}_{\circ,k}^{(\mathrm{h})})^*/\|\hat{\boldsymbol{A}}_{\circ,k}^{(\mathrm{h})}\|\} \tag{3.8}$$

where '*' is the complex conjugate operator, and '$\times$' is the cross-product operator.

Finally, the element in (3.6) whose Euclidean distance from $-\hat{\boldsymbol{u}}(\phi_k, \theta_k)$, which is given by (3.8), is the smallest yields a *low variance and unambiguous* PV estimate for the kth signal (see [10] for justifications). An estimate for the DOA of the kth signal can then be obtained directly from the PV estimate.

B. The Proposed Method—ESPRIT2$'$

First, recall that the proposed ESPRIT2$'$, which is capable of handling both CP and IP signals, is a refinement of ESPRIT2. Although ESPRIT2$'$ makes use of basically all the computations required by ESPRIT2 as proposed by Wong and Zoltowski [10], we will identify a crucial assumption that was not mentioned in [10], as well as some additional processing, and carry out necessary generalization to include more types of arrays.

1) The Data Model for ESPRIT2$'$: When CP and IP signals co-exist, we should adopt the data model as given by (2.4), where the values of p and q are not necessarily zero. Furthermore, it is worthwhile rewriting it as follows by exploiting the fact that the array of concern is a three-sensor right-triangular array

$$\begin{aligned}\boldsymbol{y}(t) = \boldsymbol{A}\boldsymbol{z}(t) + \boldsymbol{e}(t) &= [\boldsymbol{A}_\circ^T, (\boldsymbol{D}^x)^T\boldsymbol{A}_\circ^T, (\boldsymbol{D}^y)^T\boldsymbol{A}_\circ^T]^T\\ &\quad \cdot \boldsymbol{z}(t) + \boldsymbol{e}(t) \in \mathbb{C}^{18\times 1}\end{aligned} \tag{3.9}$$

where

$$\begin{aligned}\boldsymbol{A}_\circ &= [\boldsymbol{v}_1^{(\circ)}, \cdots, \boldsymbol{v}_p^{(\circ)}, \boldsymbol{v}_{\phi,p+1}^{(\circ)}, \boldsymbol{v}_{\theta,p+1}^{(\circ)}, \cdots\\ &\qquad \boldsymbol{v}_{\phi,p+q}^{(\circ)}, \boldsymbol{v}_{\theta,p+q}^{(\circ)}] \in \mathbb{C}^{6\times(p+2q)}\\ \boldsymbol{D}^x &= \text{Diag}\{e^{j2\pi\Delta u_1^x/\lambda}, \cdots, e^{j2\pi\Delta u_p^x/\lambda}, e^{j2\pi\Delta u_{p+1}^x/\lambda}\\ &\qquad e^{j2\pi\Delta u_{p+1}^x/\lambda}, \cdots, e^{j2\pi\Delta u_{p+q}^x/\lambda}, e^{j2\pi\Delta u_{p+q}^x/\lambda}\}\\ &\qquad \in \mathbb{C}^{(p+2q)\times(p+2q)}\\ \boldsymbol{D}^y &= \text{Diag}\{e^{j2\pi\Delta u_1^y/\lambda}, \cdots, e^{j2\pi\Delta u_p^y/\lambda}, e^{j2\pi\Delta u_{p+1}^y/\lambda}\\ &\qquad e^{j2\pi\Delta u_{p+1}^y/\lambda}, \cdots, e^{j2\pi\Delta u_{p+q}^y/\lambda}, e^{j2\pi\Delta u_{p+q}^y/\lambda}\}\\ &\qquad \in \mathbb{C}^{(p+2q)\times(p+2q)}.\end{aligned} \tag{3.10}$$

(See the paragraph after (2.3) for the physical meanings of $\boldsymbol{v}_k^{(\circ)}$, $\boldsymbol{v}_{\phi,k}^{(\circ)}$ and $\boldsymbol{v}_{\theta,k}^{(\circ)}$.) Although the analysis presented in [10] is carried out based on the CP signal model, we will show that it is basically valid for the model given by (3.9)–(3.10).

2) A Crucial Assumption We first consider the case where all the signals are CP. As a matter of fact, ESPRIT2 computes a set of "unambiguous" PV estimates via the cross-product technique given by (3.8). However, such PV estimates may be erroneous if Assumption 7) (stated below) is not satisfied. Indeed, we will establish in Appendix A that, upon determination of the PV estimates via the cross-product technique, Assumption 7) is a necessary and sufficient condition for ensuring that each PV estimate obtained indeed corresponds to an incoming signal.

Assumption 7) $u_k^x \ne u_l^x + i\lambda/\Delta$ for all $k, l \in \{1, \cdots, n\}$, where $k \ne l$, and for all integers i.

Remarks:

1) Assumption 7) imposes some constraints on the DOA's of the signals. For example, if there exist two incoming signals whose DOA's are reflection of each other with respect to the plane containing the three sensors of the array, then Assumption 7) is no longer valid. Moreover, the larger the intersensor spacing (i.e., Δ) is, the larger the set of DOA's leading to invalidity of Assumption 7).
2) $\hat{\boldsymbol{A}}_\circ$ can also be estimated by $\boldsymbol{E}_{s,1}\boldsymbol{G}$ instead of the expression given by (3.7), where $\boldsymbol{G} = [\boldsymbol{g}_1, \cdots, \boldsymbol{g}_n]$. In this case, Assumption 7) should be rewritten as "$u_k^y \neq u_l^y + i\lambda/\Delta$ for all $k, l \in \{1, \cdots, n\}$, where $k \neq l$ and for all integers i."

Next, we will consider the case where CP and IP signals co-exist and assuming Assumptions 1)–6) are valid. We will show that if Assumption 7) is satisfied, then determination of PV estimates via the cross-product technique [given by (3.8)] adopted by ESPRIT2 is also applicable. Indeed, let $\boldsymbol{E}_{s,1}$, $\boldsymbol{E}_{s,2}$, $\boldsymbol{E}_{s,3}$, $\boldsymbol{\Gamma}^x$, $\boldsymbol{\Gamma}^y$, f_k, $\boldsymbol{f}_k$, g_k, and $\boldsymbol{g}_k$, $k = 1, \cdots, p+2q$, be defined in a way similar to those mentioned in Section III-A. Then, it can be deduced from (2.6), (3.9), and Assumption 6) that (3.3) is still valid, where the matrices $\boldsymbol{D}^x$ and $\boldsymbol{D}^y$ are as defined in (3.10). Thus, it follows from (3.3) that f_k and g_k are, respectively, equal to the diagonal elements of $\boldsymbol{D}^x$ and $\boldsymbol{D}^y$, for $k = 1, \cdots, p+2q$. Without loss of generality, assume that

$$f_k = d_k^x \quad \text{and} \quad g_k = d_k^y, \quad \text{for } k = 1, \cdots, p+2q \tag{3.11}$$

where d_k^x and d_k^y are, respectively, the kth diagonal elements of $\boldsymbol{D}^x$ and $\boldsymbol{D}^y$. Now, let us denote

$$\tilde{\boldsymbol{A}}_\circ \triangleq \boldsymbol{E}_{s,1}\tilde{\boldsymbol{F}} \tag{3.12}$$

where $\tilde{\boldsymbol{F}} = [\boldsymbol{f}_1, \cdots, \boldsymbol{f}_{p+2q}]$. We will show that applying the cross-product technique on $\tilde{\boldsymbol{A}}_\circ$ will yield correct PV estimates. Indeed, if Assumption 7) is satisfied, then it can be shown that (see [16])

$$\begin{aligned}\tilde{\boldsymbol{A}}_\circ = [&\boldsymbol{v}_1^{(\circ)}, \cdots, \boldsymbol{v}_p^{(\circ)}, \boldsymbol{v}^{(\circ)}(\hat{\boldsymbol{\Psi}}_{p+1}), \boldsymbol{v}^{(\circ)}(\tilde{\boldsymbol{\Psi}}_{p+1}), \cdots \\ &\boldsymbol{v}^{(\circ)}(\hat{\boldsymbol{\Psi}}_{p+q}), \boldsymbol{v}^{(\circ)}(\tilde{\boldsymbol{\Psi}}_{p+q})]\boldsymbol{D}_{p+2q}\end{aligned} \tag{3.13}$$

where $\boldsymbol{D}_{p+2q}$ is a $(p+2q)$ by $(p+2q)$ diagonal matrix, $\hat{\boldsymbol{\Psi}}_{p+k} = (\phi_{p+k}, \theta_{p+k}, \hat{\gamma}_{p+k}, \hat{\eta}_{p+k})$ and $\tilde{\boldsymbol{\Psi}}_{p+k} = (\phi_{p+k}, \theta_{p+k}, \tilde{\gamma}_{p+k}, \tilde{\eta}_{p+k})$ are associated with the same DOA $(\phi_{p+k}, \theta_{p+k})$, and $(\hat{\gamma}_{p+k}, \hat{\eta}_{p+k})$, and $(\tilde{\gamma}_{p+k}, \tilde{\eta}_{p+k})$ are some unknown polarization parameters for $k = 1, \cdots, q$.

Subsequently, two deductions can be made by comparing the expression of $\tilde{\boldsymbol{A}}_\circ$ in (3.13) with that of $\boldsymbol{A}_\circ$ in (3.10). First, for $k = 1, \cdots, p$, the kth column of $\tilde{\boldsymbol{A}}_\circ$, which is associated with a CP signal, is a scalar multiple of the kth column of $\boldsymbol{A}_\circ$, and consequently, the cross product of the normalized top and bottom 3×1 subvectors of the kth column of $\tilde{\boldsymbol{A}}_\circ$ will yield an unambiguous PV estimate of the kth signal. Second, for $l = 1, \cdots, q$, the $(p+2l-1)$th and $(p+2l)$th columns of $\tilde{\boldsymbol{A}}_\circ$, which are associated with the same IP signal, are scalar multiples of a steering vector of a single VS with the same DOA $(\phi_{p+l}, \theta_{p+l})$ but with some unknown polarizations $(\hat{\gamma}_{p+l}, \hat{\eta}_{p+l})$, and $(\tilde{\gamma}_{p+l}, \tilde{\eta}_{p+l})$, respectively. Thus, for $k = p+1, \cdots, p+q$, the cross product of the normalized top and bottom 3×1 subvectors of the $(2k-p-1)$th (and $(2k-p)$th) column of $\tilde{\boldsymbol{A}}_\circ$ will yield an unambiguous PV estimate of the k signal. In summary, the two deductions mean that with Assumption 7), we can ensure that the PV estimates obtained via the cross-product technique on $\tilde{\boldsymbol{A}}_\circ$ are unambiguous for scenarios where CP and IP signals co-exist.

3) Additional Processing: We will discuss some additional processing (additional to that required by ESPRIT2 [10]) relevant to grouping of f_k's, which is necessary as far as classification of polarizations states of signals (will be discussed in Section III-B4) is concerned. Indeed, from (3.10), it is clear that the $(p+2k-1)$th and $(p+2k)$th diagonal elements of $\boldsymbol{D}^x$ are identical for $k = 1, \cdots, q$ since they are associated with an IP signal that can be viewed as one comprising two incoherent CP signals with the same DOA. Thus, we can obtain from (3.11) that $f_{p+2k-1} = f_{p+2k}$ for $k = 1, \cdots, q$. Moreover, by Assumption 7), $f_1, f_2, \cdots, f_p, f_{p+2}, f_{p+4}, \cdots, f_{p+2q}$ are all distinct. Hence, the p eigenvalues from $f_1, \cdots, f_{p+2q}$ that appear exactly once offer sensible estimates of the first p diagonal elements of $\boldsymbol{D}^x$ (the eigenvalues are $f_1, \cdots, f_p$ according to our formulation and correspond to the p CP signals), and the q distinct eigenvalues from $f_1, \cdots, f_{p+2q}$ that appear exactly twice offer estimates of the $(p+2)$th, $(p+4)$th, $\cdots$, $(p+2q)$th diagonal elements of $\boldsymbol{D}^x$ (the eigenvalues are $f_{p+2}, f_{p+4}, \cdots, f_{p+2q}$, and correspond to the q IP signals). Note that when the number of snapshots is finite, the eigenvalues $f_1, \cdots, f_{p+2q}$ will be quite distinct, strictly speaking. Nevertheless, we may take two eigenvalues to be "identical" if the difference between them is sufficiently small.

4) DOA Estimation and Polarization State Classification: Here, we first discuss estimation of a set of *low variance but ambiguous* PV's. Note that the kth diagonal elements of $\boldsymbol{D}^x$ and $\boldsymbol{D}^y$ are f_k and g_k, respectively. Since $f_{p+2k-1} = f_{p+2k}$ for $k = 1, \cdots, q$, it can be deduced from (3.10) that the candidates for u_k^x, where $k = 1, \cdots, p+q$, are given by the set

$$\tilde{S}_k^x = \left\{ \frac{\lambda}{\Delta}\left(\frac{\angle f_l}{2\pi} + \mu\right) \middle| \mu \in \boldsymbol{Z}, \left|\frac{\lambda}{\Delta}\left(\frac{\angle f_l}{2\pi} + \mu\right)\right| \leq 1 \right.$$
$$\left. l = \begin{cases} k, & \text{if } k \in [1, p], \\ 2k-p, & \text{if } k \in [p+1, p+q]. \end{cases} \right\} \tag{3.14}$$

and the candidates for u_k^y, where $k = 1, \cdots, p+q$, are given by the set

$$\tilde{S}_k^y = \left\{ \frac{\lambda}{\Delta}\left(\frac{\angle g_l}{2\pi} + \nu\right) \middle| \nu \in \boldsymbol{Z}, \left|\frac{\lambda}{\Delta}\left(\frac{\angle g_l}{2\pi} + \nu\right)\right| \leq 1 \right.$$
$$\left. l = \begin{cases} k, & \text{if } k \in [1, p], \\ 2k-p, & \text{if } k \in [p+1, p+q]. \end{cases} \right\}. \tag{3.15}$$

Now, assume that the eigenvalues of $\boldsymbol{\Gamma}^x$ and those of $\boldsymbol{\Gamma}^y$ are correctly paired (this can be done by using the method adopted by ESPRIT1 or ESPRIT2). Then, a set of *low variance but ambiguous* PV estimates for the kth signal is given by the set

$$\tilde{S}_k = \{(a, b, \pm\sqrt{1-a^2-b^2})^T | a \in \tilde{S}_k^x, b \in \tilde{S}_k^y, a^2+b^2 \leq 1\}. \tag{3.16}$$

Next, from the two deductions made in the last paragraph of Section III-B2, a *high variance but unambiguous* PV estimate of the kth signal $-\tilde{\boldsymbol{u}}(\phi_k, \theta_k)$ can be estimated by (3.17), shown at the bottom of the next page, where $\tilde{\boldsymbol{A}}_{\circ,k}^{(e)}$, and $\tilde{\boldsymbol{A}}_{\circ,k}^{(h)}$ are, respectively, the top and bottom 3×1 subvectors of the kth column of $\tilde{\boldsymbol{A}}_\circ$, as defined in (3.12).

Finally, the element in (3.16) whose Euclidean distance from $-\tilde{\boldsymbol{u}}(\phi_k, \theta_k)$ as given by (3.17) is the smallest, gives a *low variance and unambiguous* PV estimate for the kth signal. The DOA estimate of the kth signal (ϕ_k, θ_k) can be simply extracted from the PV estimate. It will be classified as the DOA of a CP signal if it is associated with an element in $\{f_1, \cdots, f_p\}$ but an IP signal if associated with an element in $\{f_{p+1}, \cdots, f_{p+2q}\}$.

In conclusion, our analysis has shown that ESPRIT2, with Assumption 7) and the additional processing we have outlined in Section III-B3, is applicable for scenarios where CP and IP signals co-exist.

5) Extension to Arbitrary Triangular Arrays: In practice, it may not be always possible to arrange three sensors in a right-triangular fashion suggested in [10] due to, for example, terrain constraint.

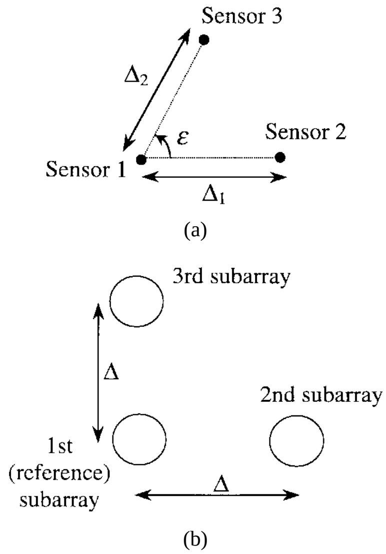

Fig. 1. (a) Three sensors inclined at an angle ε. (b) Three identical subarrays.

On the other hand, using only three sensors limits the number of identifiable signals (see Section IV for a more detailed discussion of the identifiability issues). Hence, we will generalize ESPRIT2 to allow for three-sensor arrays without the right-triangular constraint here as well as to allow for arrays with more than three sensors in Section III-B6. We will cover the desired sensor geometry as well as the relevant modification of some settings for ESPRIT2. Note that the possibility of extending ESPRIT2 to include rectangular arrays with more than three sensors has been briefly mentioned in [10], but no further details are presented.

Now, let us consider a three-sensor array as shown in Fig. 1(a). The data model is still of the form given by (3.9) and (3.10) but with the variable u_k^y of $\boldsymbol{D}^y$ in (3.10) being replaced by $[u_k^x \cos\varepsilon + u_k^y \sin\varepsilon]$ (which is effectively the projection of the PV of the kth signal onto the vector joining Sensors 1 and 3) and the variable Δ of $\boldsymbol{D}^x$ and $\boldsymbol{D}^y$ in (3.10) being replace by, respectively, Δ_1 and Δ_2. Subsequently, the whole estimation procedure presented in Sections III-B3 and 4 is applicable, except that the variable Δ of $\tilde{S}_k^x$ in (3.14) will be replaced by Δ_1, and the set $\tilde{S}_k^y$ in (3.15) will be replaced by

$$\left\{ y \triangleq \frac{\dfrac{\lambda}{\Delta_2}\left(\dfrac{\angle g_l}{2\pi} + \nu\right) - u_k^x \cos\varepsilon}{\sin\varepsilon} \,\middle|\, \nu \in \boldsymbol{Z}, u_k^x \in \tilde{S}_k^x, |y| \le 1 \quad l = \begin{cases} k, & \text{if } k \in [1, p] \\ 2k - p, & \text{if } k \in [p+1, p+q]. \end{cases} \right\}.$$

6) Extension to Arrays with More Than Three Sensors: Consider the case of arrays containing more than three sensors. The constraint is that the array must contain three identical m_{SA}-sensor subarrays (with no restriction on the value of m_{SA}), which can be overlapped. In fact, one of the subarrays is a *reference* subarray, whereas the other two are displacement versions of the reference subarray as shown in Fig. 1(b). Note that the three-sensor arrangement as required by the original ESPRIT2 as proposed in [10] may be taken as a special case of the sensor configuration we proposed here in the sense that the reference "subarray" is simply the first sensor, and the other two sensors are the displacement versions.

Without loss of generality, assume that the reference subarray contains the first m_{SA} sensors of the array. Then, the array measurements can be expressed as (3.9) and (3.10), except that the matrix $\boldsymbol{A}_\circ$ should be replaced by

$$\begin{aligned}\check{\boldsymbol{A}} = [&\check{\boldsymbol{d}}_1 \otimes \boldsymbol{v}_1^{(\circ)}, \cdots, \check{\boldsymbol{d}}_p \otimes \boldsymbol{v}_p^{(\circ)}, \check{\boldsymbol{d}}_{p+1} \otimes \boldsymbol{v}_{\phi,\,p+1}^{(\circ)}, \\ &\check{\boldsymbol{d}}_{p+1} \otimes \boldsymbol{v}_{\theta,\,p+1}^{(\circ)}, \cdots, \check{\boldsymbol{d}}_{p+q} \otimes \boldsymbol{v}_{\phi,\,p+q}^{(\circ)}, \check{\boldsymbol{d}}_{p+q} \otimes \boldsymbol{v}_{\theta,\,p+q}^{(\circ)}] \end{aligned} \tag{3.18}$$

which characterizes the response of the reference subarray due to the incoming signals, where $\check{\boldsymbol{d}}_k = [e^{j2\pi \boldsymbol{u}_k \bullet \boldsymbol{r}_1/\lambda}, \cdots, e^{j2\pi \boldsymbol{u}_k \bullet \boldsymbol{r}_{m_{\mathrm{SA}}}/\lambda}]^T$ contains the phase delays of the first m_{SA} sensors with respect to the origin. The whole estimation procedure presented in Sections III-B3 and 4 for three-sensor arrays is applicable except for two changes:

i) Assumption 6 should be replaced by Assumption $\hat{6}$.

Assumption $\hat{6}$) The columns of the matrix $\check{\boldsymbol{A}}$ are linearly independent, where $\check{\boldsymbol{A}}$ is as defined in (3.18).

ii) Now, the matrices $\boldsymbol{\Gamma}^x$ and $\boldsymbol{\Gamma}^y$ [defined in the paragraph above (3.11)] are those satisfying, respectively, $\check{\boldsymbol{E}}_{s,1}\boldsymbol{\Gamma}^x = \check{\boldsymbol{E}}_{s,2}$ and $\check{\boldsymbol{E}}_{s,1}\boldsymbol{\Gamma}^y = \check{\boldsymbol{E}}_{s,3}$, where $\check{\boldsymbol{E}}_{s,k}$ is a m_{SA}-row submatrix of $\boldsymbol{E}_s$ associated with the kth subarray (for $k = 1, 2, 3$), and each row of $\check{\boldsymbol{E}}_{s,k}$ is extracted from a row of $\boldsymbol{E}_s$ corresponding to a sensor of the kth subarray.

Remark: If the three subarrays are not inclined at right angle, then the modification required for arbitrary triangular arrangements as discussed in Section III-B5 should also be carried out.

IV. Identifiability Issues

Since identifiability is a subject by itself and not the only issue of this correspondence, we will present only the relevant results here while putting detailed analysis in the Appendix. For ease of discussion, we introduce a tight bound (tight in the sense that it is relatively tighter than the loose bound that we will shortly discuss) denoted as $n_{\mathrm{ESP}}^{\mathrm{t}}$ and a loose bound $n_{\mathrm{ESP}}^{\mathrm{l}}$, where $n_{\mathrm{ESP}}^{\mathrm{t}}$ and $n_{\mathrm{ESP}}^{\mathrm{l}}$ are both positive integers, and $n_{\mathrm{ESP}}^{\mathrm{l}} > n_{\mathrm{ESP}}^{\mathrm{t}}$. We will first discuss the implications of $n_{\mathrm{ESP}}^{\mathrm{t}}$ and $n_{\mathrm{ESP}}^{\mathrm{l}}$ and later on present their values. Indeed, our investigation reveals that when $n = p + q < n_{\mathrm{ESP}}^{\mathrm{t}}$, where n is the total number of signals, p is the number of CP signals, and q is the number of IP signals, the DOA estimates obtained with ESPRIT2$'$ will be unique and valid (valid here means that it is indeed the DOA of an incoming signal if all desired assumptions [i.e., Assumptions 1)–7)] are satisfied). In the case where $n_{\mathrm{ESP}}^{\mathrm{t}} \le n \le n_{\mathrm{ESP}}^{\mathrm{l}}$, some of the DOA estimates could be invalid depending the DOA's of the incoming signals. Beyond $n_{\mathrm{ESP}}^{\mathrm{l}}$, none of the estimates would be valid.

Our study first establishes that $n_{\mathrm{ESP}}^{\mathrm{t}} = 2$ and $n_{\mathrm{ESP}}^{\mathrm{l}} = 6m_{\mathrm{SA}} - q$, where $q \in [0, 3m_{\mathrm{SA}}]$, and m_{SA} is the number of VS's in each

$$-\tilde{\boldsymbol{u}}(\phi_k, \theta_k) = \begin{cases} -\mathrm{Re}\left\{ \dfrac{\tilde{\boldsymbol{A}}_{\circ,k}^{(\mathrm{e})}}{\|\tilde{\boldsymbol{A}}_{\circ,k}^{(\mathrm{e})}\|} \times \dfrac{(\tilde{\boldsymbol{A}}_{\circ,k}^{(\mathrm{h})})^*}{\|\tilde{\boldsymbol{A}}_{\circ,k}^{(\mathrm{h})}\|} \right\}, & \text{if } k = 1, \cdots, p \\ -\dfrac{1}{2}\,\mathrm{Re}\left\{ \dfrac{\tilde{\boldsymbol{A}}_{\circ,2k-p}^{(\mathrm{e})}}{\|\tilde{\boldsymbol{A}}_{\circ,2k-p}^{(\mathrm{e})}\|} \times \dfrac{(\tilde{\boldsymbol{A}}_{\circ,2k-p}^{(\mathrm{h})})^*}{\|\tilde{\boldsymbol{A}}_{\circ,2k-p}^{(\mathrm{h})}\|} \right\} - \dfrac{1}{2}\,\mathrm{Re}\left\{ \dfrac{\tilde{\boldsymbol{A}}_{\circ,2k-1-p}^{(\mathrm{e})}}{\|\tilde{\boldsymbol{A}}_{\circ,2k-1-p}^{(\mathrm{e})}\|} \times \dfrac{(\tilde{\boldsymbol{A}}_{\circ,2k-1-p}^{(\mathrm{h})})^*}{\|\tilde{\boldsymbol{A}}_{\circ,2k-1-p}^{(\mathrm{h})}\|} \right\}, & \text{if } k = p+1, \cdots, p+q \end{cases} \tag{3.17}$$

subarray (see Appendix B). Clearly, the loose bound $n^1_{\rm ESP}$ depends on q, which is the number of IP signals. Indeed, it can be verified that it takes one extreme value $6m_{\rm SA}$ when $q = 0$ (which corresponds to the case where there is no IP signals) and the other extreme value $3m_{\rm SA}$ when $q = 3m_{\rm SA}$ (which corresponds to the case where there is no CP signals).

Remarks:

1) From the loose bound $n^1_{\rm ESP} = 6m_{\rm SA} - q$, we can deduce that by increasing the number of sensors, $n^1_{\rm ESP}$ increases, and ESPRIT2$'$ can potentially handle more signals. For example, consider the case where all the signals are CP. Then, for a three-sensor array, ESPRIT2$'$ can handle up to six signals. On the other hand, for a six-sensor array comprising three subarrays with each subarray having two sensors arranged in a way described in Section III-B6, ESPRIT2$'$ can handle up to 12 signals.
2) If the number of signals is between the loose and tight bounds, there is a set of DOA's, whereby Assumption $\hat{6}$) or 7) is violated, leading to some ambiguous estimates. However, such a set of DOA's is of measure zero, i.e., there would be practically no ambiguity when the SNR is sufficiently high. In addition, by increasing the number of sensors, we can reduce the size of the ambiguity since fewer DOA combinations would lead to invalidity of Assumption $\hat{6}$).
3) It is also possible to eliminate ambiguities arise due to violation of Assumption 7) [assuming Assumptions 1)–5) and $\hat{6}$) are satisfied]. Here, we will briefly outline a method exploiting the fact that the signal subspace is orthogonal to the noise subspace. Indeed, to obtain unique DOA estimates, we first carry out the first part of ESPRIT2$'$ involving the computation of a set of *low variance but ambiguous* PV estimates $\tilde{S}_k$ for $k = 1, \cdots, p+q$, which are given by (3.16). To remove ambiguous PV estimates, we will not proceed with the second part of ESPRIT2$'$ involving the computation of the *high variance but unambiguous* PV estimates [given by (3.17)] but carry out the procedure as follows. Let us first denote the set of DOA's associated with the set of PV estimates in $\tilde{S}_k$ as $\Omega_k \triangleq \{(\phi, \theta) | \phi = \tan^{-1}(y/x),\ \theta = \sin^{-1}(z),\ (x, y, z) \in \tilde{S}_k\}$. Now, using the fact that the signal subspace is orthogonal to the noise subspace, the DOA $(\phi_k,\ \theta_k)$ associated with the k signal can be uniquely determined via $\arg\min_{(\phi,\theta)\in\Omega_k}\ \lambda_{\min}([\boldsymbol{v}_\phi(\phi,\theta), \boldsymbol{v}_\theta(\phi,\theta)]^H \boldsymbol{E}_n \boldsymbol{E}_n^H [\boldsymbol{v}_\phi(\phi,\theta), \boldsymbol{v}_\theta(\phi,\theta)])$, where $\lambda_{\min}(\boldsymbol{X})$ denotes the smallest eigenvalue of $\boldsymbol{X}$, and $\boldsymbol{E}_n$ is the noise subspace defined in (2.5).

V. Simulation Results

We present numerical examples to demonstrate the effectiveness of ESPRIT2$'$. In each example, we generate 100 Monte Carlo runs, and for each run, 100 snapshots are generated. The default values of the signal-to-noise ratios (SNR's) are 10 dB, unless otherwise stated. The array comprises three VS's with coordinates (0, 0, 0), (Δ, 0, 0) and (0, Δ, 0), where $\Delta = 2\lambda$. We compare the performance of ESPRIT2$'$ with a form of CRB, RMSAE$_{\rm CR}$,[1] which is defined as RMSAE$_{\rm CR} \triangleq \sqrt{\cos^2\theta\,{\rm CRB}(\phi) + {\rm CRB}(\theta)}$, where ${\rm CRB}(\phi)$ and ${\rm CRB}(\theta)$ are the CRB's for the azimuth and elevation, respectively (see [2, (3.4)]). In fact, RMSAE$_{\rm CR}$ provides a lower bound for the root-mean-square angular errors (RMSAE's) of DOA (azimuth and elevation) estimates.

Before we proceed, we will introduce the degree of polarization (DOP) of a signal. The covariance matrix of the kth signal $\boldsymbol{R}_{\boldsymbol{\rho}_k}$ can be expressed as $\sigma^2_{k,\rm UP}\boldsymbol{I}_2/2 + \sigma^2_{k,\rm CP}[\cos\gamma_k, \sin\gamma_k e^{i\eta_k}]^T[\cos\gamma_k, \sin\gamma_k e^{-i\eta_k}]$, where $\sigma^2_{k,\rm UP}, \sigma^2_{k,\rm CP} \in \Re$, $\gamma_k \in [0, \pi/2]$, $\eta_k \in (-\pi, \pi]$, and $\boldsymbol{I}_2$ is the (2×2) identity matrix [15]. The first term is the unpolarized (UP) component with power $\sigma^2_{k,\rm UP}$, and the second is the CP component with power $\sigma^2_{k,\rm CP}$. The DOP of the signal is defined as the ratio between the power of the CP component and the total power of the signal, i.e., $\sigma^2_{k,\rm CP}/(\sigma^2_{k,\rm UP} + \sigma^2_{k,\rm CP})$. Note that the value of DOP ranges from 0 to 1, with the DOP of a CP signal being 1, and that of an IP signal being less than 1. A special case of an IP signal that has no CP component is called a UP signal, and its DOP is 0.

[1] RMSAE$_{\rm CR}$ is based on the mean-square angular error as defined in [2].

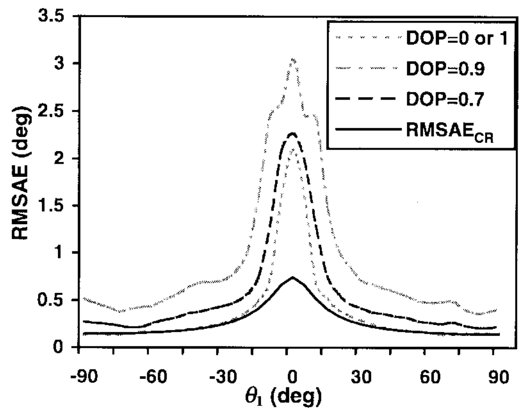

Fig. 2. RMSAE's of the estimates of ESPRIT2$'$ and RMSAE$_{\rm CR}$ for scenarios of one signal. The signal parameters are $(\phi_1, \theta_1, \gamma_1, \eta_1) = (45°, \theta_1, 0°, 0°)$, where θ_1 is varied from -90 to 90°, and the DOP is varied from 0 to 1. (Note that RMSAE$_{\rm CR}$ is the CRB for the case DOP $=$ 0, and the RMSAE for DOP $= 0$ is almost identical to that when DOP $=$ 1.)

In the first example, we assess the performance of ESPRIT2$'$ in the presence of one signal. We simulate one signal with parameter $\boldsymbol{\Psi}_1 = (45°, \theta_1, 0°, 0°)$, where the elevation θ_1 is varied from $-90°$ to 90° in steps of 5°. The DOP of the signal under investigation ranges from 0 to 1. The results are shown in Fig. 2. When DOP $=$ 0 or 1, the RMSAE of the DOA estimates is close to RMSAE$_{\rm CR}$ if $|\theta| > 10°$ (i.e., $\theta < -10°$ or $\theta > 10°$). The large value of the RMSAE at low elevation (i.e., $|\theta| \le 10°$) is due to the fact that all the three sensors lie in the x-y plane (better results can be expected if there are sensors not confined in the x-y plane). When we vary the DOP of the signal from 0 to 1 in steps of 0.1, the RMSAE of the DOA estimates increases gradually as the DOP of the signal increases from 0 to 0.9. Interestingly, as the DOP increases further from 0.9 to 1, the RMSAE decreases from the maximum value attained at DOP equal to 0.9 to a value close to that when the DOP is 0. The above observations indicate that ESPRIT2$'$ works best at the two extreme polarizations, i.e., CP or UP, but not in between.

In the second example, we are concerned with the dependence of the performance on the angular separation of two signals. We simulate two uncorrelated signals of which the first is CP with parameters fixed at $\boldsymbol{\Psi}_1 = (45°, -65°, 0°, 0°)$, and the second is UP with parameters $\boldsymbol{\Psi}_2 = (45°, -65° + \delta, 90°, 0°)$, where δ is varied from 0 to 155° in steps of 5°. The result associated with the first signal is shown in Fig. 3. Clearly, the RMSAE of the DOA estimates decreases with an increase in angular separation, except for the case where $\delta = 130°$ (the violation of Assumption 7 when $\delta = 130°$ has led to large RMSAE). As to the case where $\delta = 130°$, we can apply the processing proposed in Remark iii) of Section IV to obtain an estimate with RMSAE being close to RMSAE$_{\rm CR}$. Note that we also show in Fig. 3 (and in Fig. 4 as well for the next example) the RMSAE of the high variance DOA estimates obtained from (3.17). Apparently, the RMSAE of the high variance estimates is

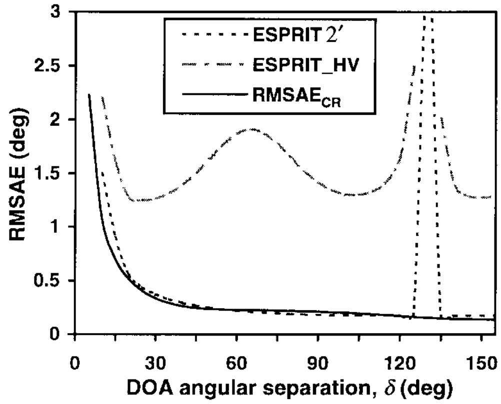

Fig. 3. RMSAE of the DOA estimates of the first signal versus DOA angular separation δ for scenarios where 1 CP and 1 UP signals co-exist. The parameters of the CP signal are fixed at $(\phi_1, \theta_1, \gamma_1, \eta_1) = (45°, -65°, 0°, 0°)$, and those of the UP signal are $(\phi_2, \theta_2, \gamma_2, \eta_2) = (45°, -65° + \delta, 90°, 0°)$. "ESPRIT_HV" in the legend corresponds to high variance estimate of ESPRIT2$^{'}$.

much higher than that obtained through the combination of both the high-variance and low-variance estimates.

In the third example, we investigate the dependence of the performance on SNR in the presence of two signals. We simulate two uncorrelated signals of which the first is CP with parameters fixed at $\boldsymbol{\Psi}_1 = (45°, -60°, 0°, 0°)$, and the second is UP with parameters fixed at $\boldsymbol{\Psi}_2 = (45°, -30°, 90°, 0°)$. The SNR's of the two signals are equal and are concurrently varied from -2 to 20 dB in steps of 1 dB. The results associated with the first and second signals are shown in Fig. 4(a) and (b), respectively. We observe that the RMSAE of the DOA estimates increases with a decrease in SNR, and moreover, it is close to RMSAE_{CR}.

Next, we discuss the ability to accurately determine which of the signals are CP and which are not. Tables I and II show the percentage of erroneous classifications that have occurred for the second and third examples, respectively. We observe that incorrect classifications often occur when angular separation between signals is small or SNR is low. We also notice that very often, when there is a large percentage of incorrect classifications, the DOA estimates are all quite poor (see Figs. 3 and 4). Incidentally, there was no incident of incorrect classification in the entire process of Example 1. One main reason is that Example 1 involves only one signal, and the SNR value is considerably high.

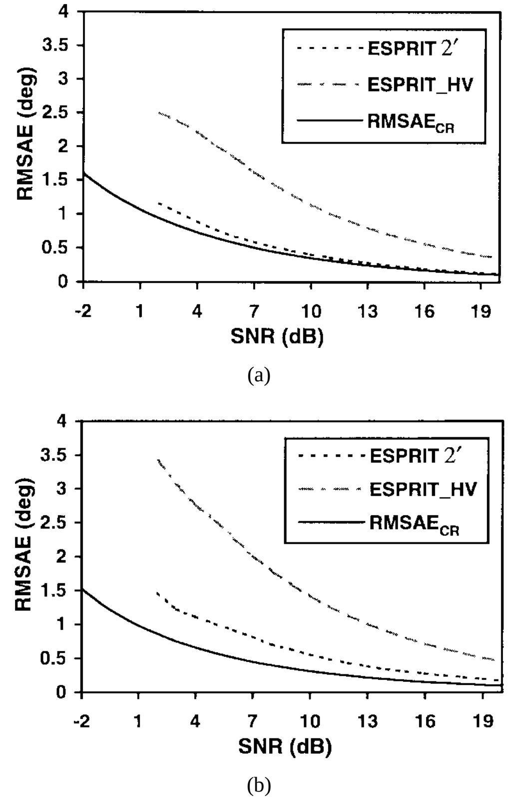

Fig. 4. (a) RMSAE of the DOA estimates of the first signal versus SNR for scenarios of two signals. The first signal is CP with $(\phi_1, \theta_1, \gamma_1, \eta_1) = (45°, -60°, 0°, 0°)$, and the second is UP with $(\phi_2, \theta_2, \gamma_2, \eta_2) = (45°, -30°, 90°, 0°)$. (b) As in Fig. 4(a), but this figure shows the RMSAE of the DOA estimates of the second signal.

TABLE I

Erroneous Classification (EC) of Polarization States in the Second Example for DOA Angular Separation, δ. (Angular Separations that are Not Shown Do Not Have Erroneous Classifications)

δ (deg)	0	5	10	130
EC (%)	100	62	16	100

TABLE II

Erroneous Classification (EC) of Polarization States in the Third Example. (SNR's that Are Not Shown Do Not Have Erroneous Classifications)

SNR(dB)	−2	−1	0	1	2	3
EC (%)	100	100	54	42	19	13

VI. Summary

We addressed DOA estimation with EM VS's for scenarios where CP and IP signals co-exist. Although there had been existing methods for estimating the DOA's of multiple signals with an array of EM VS's, they had been designed either for only CP signals or for only IP signals. The fact that a method suitable for CP (IP) signals may fail completely in the presence of IP (CP) signals motivated our investigation into the applicability of ESPRIT2 [10] that was designed based on CP signal model for scenarios where the two types of signals co-exist.

Our investigation showed that ESPRIT2, with an additional assumption and some extra processing, is capable of yielding reasonably good estimates of the DOA's of both CP and IP signals and of offering sensible classification of the signal types. Since ESPRIT2 was originally designed for use with a specific three-sensor array [10], we carried out an appropriate generalization to include more general types of three-sensor arrays and a class of array with an arbitrary number of EM VS's. We also acquired some useful insights into the identifiability issues concerning our proposed ESPRIT.

Appendix A
The Significance of Assumption 7

We will first establish a useful lemma.

Lemma A.1: Let $\boldsymbol{v}^{(\circ)}(\phi_k, \theta_k, \gamma_k, \eta_k)$ and $\boldsymbol{v}^{(\circ)}(\phi_l, \theta_l, \gamma_l, \eta_l)$ be two steering vectors of a single VS associated with two CP signals, where $\boldsymbol{v}^{(\circ)}$ is as defined in (2.3). If $\delta_k \boldsymbol{v}^{(\circ)}(\phi_k, \theta_k, \gamma_k, \eta_k) + \delta_l \boldsymbol{v}^{(\circ)}(\phi_l, \theta_l, \gamma_l, \eta_l) = \delta \boldsymbol{v}^{(\circ)}(\phi_k, \theta_k, \gamma, \eta)$ for some polarization (γ, η) and $\delta_k,\ \delta_l,\ \delta \in \mathbb{C}\backslash\{0\}$, then the two DOA's $(\phi_k,\ \theta_k)$ and $(\phi_l,\ \theta_l)$ are identical.

Proof of Lemma A.1: If $\delta_k \boldsymbol{v}^{(\circ)}(\phi_k, \theta_k, \gamma_k, \eta_k) + \delta_l \boldsymbol{v}^{(\circ)}(\phi_l, \theta_l, \gamma_l, \eta_l) = \delta \boldsymbol{v}^{(\circ)}(\phi_k, \theta_k, \gamma, \eta)$ for some polarization (γ, η) and $\delta_k, \delta_l, \delta \in \mathbb{C}\backslash\{0\}$, then we can rewrite the equation as $\delta_l \boldsymbol{v}^{(\circ)}(\phi_l, \theta_l, \gamma_l, \eta_l) = \delta \boldsymbol{v}^{(\circ)}(\phi_k, \theta_k, \gamma, \eta) - \delta_k \boldsymbol{v}^{(\circ)}(\phi_k, \theta_k, \gamma_k, \eta_k) = \hat{\delta} \boldsymbol{v}^{(\circ)}(\phi_k, \theta_k, \hat{\gamma}, \hat{\eta})$ for some $\hat{\gamma} \in [0, \pi/2]$, $\hat{\eta} \in (-\pi, \pi]$, and $\hat{\delta} \in \mathbb{C}\backslash\{0\}$. Now, using the fact that every two steering vectors of one VS associated with two CP signals having distinct DOA's are linear independent (see Lemma 1 of [3]), the DOA's (ϕ_k, θ_k) and (ϕ_l, θ_l) must be identical. ■

Now, we are ready to show that Assumption 7) is a necessary and sufficient condition for the cross-product method given by (3.8) yielding correct PV estimates. We begin by showing the sufficiency part, i.e., if Assumption 7) is satisfied, then (3.8) will give correct PV estimates. Indeed, if Assumption 7) is satisfied, then the diagonal elements of $\boldsymbol{D}^x$, as defined in (3.2), are all distinct. Thus, it follows from (3.4) that the eigenvalues of $\boldsymbol{\Gamma}^x$ (i.e., f_k, for $k = 1, \cdots, n$) must be all distinct. This in turn implies that $\boldsymbol{f}_k$ is a scalar multiple of the kth column of $\boldsymbol{T}$, as defined in (2.6). Consequently, it can be verified from (2.6) and (3.7) that the kth column of $\hat{\boldsymbol{A}}_\circ$, as defined in (3.7), is indeed a scalar multiple of the kth column of $\boldsymbol{A}_\circ$. Since the kth column of $\boldsymbol{A}_\circ$ is a steering vector of a single VS with DOA identical to that of the kth signal, the cross-product technique in (3.8) will yield a correct PV estimate of the kth signal.

Next, we will establish the necessity part, i.e., if Assumption 7) is violated, then (3.8) will give erroneous PV estimates. Indeed, if Assumption 7) is violated, then there exist u_k^x and u_l^x, where $k \neq l$ such that $u_k^x = u_l^x + i\lambda/\Delta$ for some integer i. Without loss of generality, we may assume that $k = 1$ and $l = 2$. It can then be deduced that $d_1^x = d_2^x$, where d_1^x and d_2^x are, respectively, the first and second diagonal elements of $\boldsymbol{D}^x$. It thus follows from (3.4) that the eigenvalues f_1 and f_2 of $\boldsymbol{\Gamma}^x$ are identical. This implies that both the eigenvectors $\boldsymbol{f}_1$ and $\boldsymbol{f}_2$ of $\boldsymbol{\Gamma}^x$ are linear combinations of the first two columns of $\boldsymbol{T}$, i.e., $\boldsymbol{f}_1 = \zeta_1 \boldsymbol{t}_1 + \zeta_2 \boldsymbol{t}_2$ and $\boldsymbol{f}_2 = \epsilon_1 \boldsymbol{t}_1 + \epsilon_2 \boldsymbol{t}_2$ for some ζ_1, ζ_2, ϵ_1, and $\epsilon_2 \in \mathbb{C}$, where $\boldsymbol{t}_1$ and $\boldsymbol{t}_2$ are the first and second columns of $\boldsymbol{T}$, respectively. Now, we note that the probability of $\boldsymbol{f}_1$ or $\boldsymbol{f}_2$ being scalar multiples of $\boldsymbol{t}_1$ or $\boldsymbol{t}_2$ (this happens when one of ζ_1 or ζ_2 is zero and one of ϵ_1 or ϵ_2 is zero) is *zero*. Therefore, it is reasonable to assume that $\boldsymbol{f}_1$ and $\boldsymbol{f}_2$ are not scalar multiples of $\boldsymbol{t}_1$ or $\boldsymbol{t}_2$. With this, it can be verified from (2.6) and (3.7) that the first (and second) column of $\hat{\boldsymbol{A}}_\circ$ is a linear combination, but not a scalar multiple, of the first and second columns of $\boldsymbol{A}_\circ$. Since the DOA's associated with the first and second columns of $\boldsymbol{A}_\circ$ are distinct (by Assumption 1), it follows from Lemma A.1 that the first (and second) column of $\hat{\boldsymbol{A}}_\circ$ is not a scalar multiple of a steering vector of a single VS having the same DOA as the first signal [i.e., (ϕ_1, θ_1)] or second signal [i.e., (ϕ_2, θ_2)]. Hence, the cross-product technique, as given by (3.8), will yield erroneous PV estimates for the first and second signals.

Appendix B
Derivation of the Tight & Loose Bounds for ESPRIT2′

We will first show that $n_{\text{ESP}}^{\text{t}} = 2$. Note that if the DOA's of two incoming signals are reflection of each other with respect to the plane containing the two displacement vectors of the second and third subarrays from the reference subarray, then Assumption 7) is no longer valid. As a result, the DOA estimates are no longer correct (see Appendix A for justifications). Thus, we have established that $n_{\text{ESP}}^{\text{t}} \leq 2$. Next, note that if there is only one signal, Assumptions $\hat{6}$) and 7) are clearly valid. Assumption $\hat{6}$) being valid means that the PV associated with the incoming signal is contained in the set of PV estimates given by (3.16). On the other hand, Assumption 7) is valid means that (3.17) will yield the correct PV estimate (see Appendix A for justifications). Thus, the PV estimate of ESPRIT2′, which is obtained from finding the PV estimate in (3.16) that is closest to that in (3.17) is identical to the PV of the incoming signal. This establishes $n_{\text{ESP}}^{\text{t}} = 2$.

Next, we will show that $n_{\text{ESP}}^{\text{l}} = 6m_{\text{SA}} - q$, where $q \in [0, 3m_{\text{SA}}]$ for an array receiving p CP signals and q IP signals. Indeed, we first note that if Assumption $\hat{6}$) is violated, then (3.3) is no longer valid. Consequently, none of the PV estimates in (3.16) is equal to the PV's of the incoming signals. Thus, it suffices to establish that if the number of incoming signals n is greater than $6m_{\text{SA}} - q$, then Assumption $\hat{6}$) is violated, regardless of the DOA's of the incoming signals. Indeed, if $n > 6m_{\text{SA}} - q$, then the number of columns of the matrix $\check{\boldsymbol{A}}$ (associated with the reference subarray), $p + 2q$, is greater than its number of rows, $6m_{\text{SA}}$. Consequently, the columns of $\check{\boldsymbol{A}}$ are linearly dependent, and Assumption $\hat{6}$) is violated regardless of the DOA's of the incoming signals.

Acknowledgment

We thank the reviewers for their insightful comments that have been very useful in strengthening the paper.

References

[1] A. Nehorai and E. Paldi, "Vector sensor processing for electromagnetic source localization," in *Proc. 25th Asilomar Conf. Signals, Syst. Comput.*, Pacific Grove, CA, 1991, pp. 566–572.

[2] ——, "Vector-sensor array processing for electromagnetic source localization," *IEEE Trans. Signal Processing*, vol. 42, pp. 376–398, Feb. 1994.

[3] K.-C. Tan, K.-C. Ho, and A. Nehorai "Linear independence of steering vectors of an electromagnetic vector sensor," *IEEE Trans. Signal Processing*, vol. 44, pp. 3099–3107, Dec. 1996.

[4] ——, "Uniqueness study of measurements obtainable with arrays of electromagnetic vector sensors," *IEEE Trans. Signal Processing*, vol. 44, pp. 1036–1039, Apr. 1996.

[5] K.-C. Ho, K.-C. Tan, and W. Ser, "An investigation on number of signals whose directions-of-arrival are uniquely determinable with an electromagnetic vector sensor," *Signal Process.*, vol. 47, no. 1, pp. 41–54, Nov. 1995.

[6] B. Hochwald and A. Nehorai, "Identifiability in array processing models with vector-sensor applications," *IEEE Trans. Signal Processing*, vol. 44, pp. 83–95, Jan. 1996.

[7] G. F. Hatke, "Conditions for unambiguous source localization using polarization diverse arrays," in *Proc. 27th Asilomar Conf. Signals, Syst. Comput.*, Los Alamitos, CA, 1993, pp. 1365–1369.

[8] ——, "Performance analysis of the SuperCART antenna array," Project Rep. AST-22, Mass. Inst. Technol. Lincoln Lab., Lexington, Mar. 1992.

[9] J. Li, "Direction and polarization estimation using arrays with small loops and short dipoles," *IEEE Trans. Antennas Propagat.*, vol. 41, pp. 379–387, Mar. 1993.

[10] K. T. Wong and M. D. Zoltowski, "High accuracy 2D angle estimation with extended aperture vector sensor arrays," *Proc. ICASSP*, May 1996, vol. 5, pp. 2789–2792.

[11] K.-C. Ho, K.-C. Tan, and B. T. G. Tan, "Estimation of directions-of-arrival of partially polarized signals with electromagnetic vector sensors," *Proc. ICASSP*, May 1996, vol. 5, pp. 2900–2903.

[12] ——, "Efficient method for estimating directions-of-arrival of partially polarized signals with electromagnetic vector sensors," *IEEE Trans. Signal Processing*, vol. 45, pp. 2485–2498, Oct. 1997.

[13] K.-C. Ho, K.-C. Tan, and A. Nehorai, "Estimation of directions-of-arrival of completely polarized and incompletely polarized signals with electromagnetic vector sensors," in *Proc. IFAC Symp. Syst. Ident.*, July 1997, vol. 2, pp. 523–528.

[14] E. R. Ferrara, Jr., and T. M. Parks, "Direction finding with an array of antennas having diverse polarizations," *IEEE Trans. Antennas Propagat.*, vol. AP-31, pp. 231–236, Mar. 1983.

[15] B. Hochwald and A. Nehorai, "Polarimetric modeling and parameter estimation with applications to remote sensing," *IEEE Trans. Signal Processing*, vol. 43, pp. 1923–1935, Aug. 1995.

[16] K.-C. Ho, K.-C. Tan, and A. Nehorai, "Estimating directions of arrival of completely and incompletely polarized signals with electromagnetic vector sensors" Report UIC-EECS-97-2, Dept. Elect. Eng. Comput. Sci., Univ. Illinois at Chicago, Apr. 1997.